

ARTICLE

Received 2 Sep 2016 | Accepted 1 Dec 2016 | Published 31 Jan 2017

DOI: 10.1038/ncomms14190

OPEN

Synthesis of ketones from biomass-derived feedstock

Qinglei Meng¹, Minqiang Hou¹, Huizhen Liu^{1,2}, Jinliang Song¹ & Buxing Han^{1,2}

Cyclohexanone and its derivatives are very important chemicals, which are currently produced mainly by oxidation of cyclohexane or alkylcyclohexane, hydrogenation of phenols, and alkylation of cyclohexanone. Here we report that bromide salt-modified Pd/C in H₂O/CH₂Cl₂ can efficiently catalyse the transformation of aromatic ethers, which can be derived from biomass, to cyclohexanone and its derivatives via hydrogenation and hydrolysis processes. The yield of cyclohexanone from anisole can reach 96%, and the yields of cyclohexanone derivatives produced from the aromatic ethers, which can be extracted from plants or derived from lignin, are also satisfactory. Detailed study shows that the Pd, bromide salt and H₂O/CH₂Cl₂ work cooperatively to promote the desired reaction and inhibit the side reaction. Thus high yields of desired products can be obtained. This work opens the way for production of ketones from aromatic ethers that can be derived from biomass.

¹Beijing National Laboratory for Molecular Sciences, CAS Key Laboratory of Colloid and Interface and Thermodynamics, Institute of Chemistry, Chinese Academy of Sciences, Beijing 100190, China. ²School of Chemistry and Chemical Engineering, University of Chinese Academy of Sciences, Beijing 100049, China. Correspondence and requests for materials should be addressed to H.L. (email: liuhz@iccas.ac.cn) or to B.H. (email: hanbx@iccas.ac.cn).

Cyclohexanone is a key raw material for producing nylon 6 and nylon 66 and for synthesis of other chemicals¹. The industrial production of cyclohexanone typically involves either the oxidation of cyclohexane² or the hydrogenation of phenol³. Cyclohexanone derivatives are also useful chemicals or intermediates to produce valuable chemicals. For example, methylcyclohexanone is used for preparing cyclohexanone imines, which can be followed by dehydrogenative aromatization to generate arylamines that are the core structures of various functional molecules with biological activities and optoelectronic properties relevant to pharmaceuticals and materials science, respectively⁴. 4-Propylcyclohexanone is used for the synthesis of chiral tacrine analogues which show important pharmacological activities⁵. The conventional synthesis of cyclohexanone derivatives typically involves either the oxidation of alkylcyclohexane⁶ or the alkylation of cyclohexanone⁷.

Utilization of biomass as raw materials to produce useful chemical compounds can liberate us from the reliance on fossil resource, and can also be considered as recycling of CO₂ by combination of photosynthesis and chemical methods⁸. Lignocellulosic biomass is abundant renewable carbon resource, and lignin is the main constituent of lignocellulosic biomass^{9,10}. However, lignin has nearly not been used in industry, especially for producing valuable compounds¹¹. It is well known that lignin is rich in aromatic ether segments and aromatic ether bonds widely exist in the structure of lignin¹². In recent years, much attention has been paid to the depolymerization of lignin, and various useful products and platform molecules have been obtained, such as liquid fuels^{13,14}, alcohols^{10,15}, and aromatic ethers^{15–20}. It can be expected that more feasible methods will be developed to produce various aromatic ethers from lignin. Moreover, aromatic ethers, such as anethole, *trans*-anethole, exist widely in plants and can be directly extracted^{21–23}. The representative aromatic ethers depicted in Fig. 1 illustrates that the natural aromatic carbon-oxygen (C_{aromatic}-O) bonds may directly provide structural integrity for the ketone-type structure of cyclohexanone by means of catalytic valorization⁹. Runnebaum *et al.*²⁴ performed the conversion of anisole in the presence of H₂ on Pt/Al₂O₃ catalyst at 300 °C, generating cyclohexanone with a selectivity of 3% and trace amounts of 2-methylcyclohexanone. Hubert *et al.*²⁵ carried out the hydrogenation of anisole using THEA16Cl-stabilized Rh (0) nanoparticles as catalyst, and the yield of cyclohexanone reached 22%.

It can be anticipated that cyclohexanone and its derivatives can be produced in sustainable way if we can develop efficient protocols to transform aromatic ethers into these important chemicals, as shown in Fig. 1. However, achieving high yield is a great challenge because aromatic ethers tend to completely hydrogenated to alkyl ethers, and ketone products can be further hydrogenated to cyclohexanol and its derivatives under the reaction conditions. Up to now, only the transformation of anisole to cyclohexanone has been reported, and the highest yield was 22%. In this work, we developed a route for the production of cyclohexanone and its derivatives from

aromatic ethers. It was discovered that bromide salt modified Pd/C (m-Pd/C) catalyst in H₂O/CH₂Cl₂ medium was highly efficient for the transformation of aromatic ethers to ketones, and the yield of cyclohexanone could reach 96% for the conversion of anisole to cyclohexanone. This catalytic system could also be applied to transform other aromatic ethers to ketones with high yields. This work opens the way for sustainable producing ketones from bio-based feedstocks.

Results

Catalytic system screening. We first used anisole to study the conversion of aromatic ethers to cyclohexanone and its derivatives because it has only one methoxy group that simplifies the study of the reaction. Commercial Pd/C catalyst (Supplementary Fig. 1) was used because it is a very commonly used catalyst for hydrogenation reactions. Table 1 presents the results of the conversion of anisole under different conditions. The reaction in different solvents was studied using Pd/C as the catalyst. Cyclohexyl methyl ether (3) was the only product in organic solvents (Table 1, entries 1–4). Cyclohexanone (1), cyclohexanol (2), and cyclohexyl methyl ether (3) were produced in water, and the selectivity to cyclohexanone (1) was 13.0% at 99.8% conversion of anisole (Table 1, entry 5), indicating that water was essential for the generation of cyclohexanone. As expected, the reaction did not occur without catalyst and/or H₂ (Table 1, entry 6). We also performed the reaction using Pt/C, Ru/C and Rh/C catalysts in water (Table 1, entries 7–9). Under the similar conversion of anisole, only 1.5% yield of cyclohexanone was obtained over Pt/C catalyst, while selectivity of the by-product cyclohexyl methyl ether (3) was higher than 80% (Table 1, entry 7). Especially, in the presence of Ru/C and Rh/C catalysts, no cyclohexanone was detected (Table 1, entries 8–9). The results above indicate that Pd/C is the best catalyst among the catalysts checked for the transformation of anisole to cyclohexanone. Considering the solubility of the solvent, some binary solvents containing water and organic solvent were used for the reaction, and H₂O/CH₂Cl₂ exhibited the best performance for producing cyclohexanone (Table 1, entries 10–12), and the yield of cyclohexanone reached 67.7%. It has been reported that small amount of halide anions could improve the selectivity of some reactions over Pd catalyst^{26,27}. Therefore, to further improve the yield of cyclohexanone, the effect of some halide salts on the reaction was studied (Table 1, entries 13–18). Similarly, cyclohexanone was not formed without water (Table 1, entry 13). All the salts with Br[−] (KBr and NaBr) could enhance the selectivity to cyclohexanone effectively in water or H₂O/CH₂Cl₂ (Table 1, entries 14–16), and particularly high selectivity could be obtained when H₂O/CH₂Cl₂ was used as the solvent. However, KCl could not improve the selectivity considerably (Table 1, entry 17). In addition, KI completely prohibited the conversion of anisole (Table 1, entry 18), which is consistent with the argument that I[−] can deactivate Pd catalyst seriously^{28,29}.

To study the reason for the high selectivity of the desired product, some control experiments (Supplementary Fig. 2) were conducted. Supplementary Fig. 2a demonstrates the dependence of yields of the products on reaction time in neat water over Pd/C. Cyclohexanone and cyclohexyl methyl ether are the main products in 1.5 h. However, the selectivity of cyclohexanone decreased quickly after 1.5 h, accompanying the increase of the selectivity of cyclohexanol because Pd can catalyse the hydrogenation of cyclohexanone to cyclohexanol³. To explain this result, we calculated the adsorption energy of anisole and cyclohexanone on Pd (111) surface by density function theory (DFT) method^{30–32}, and the values are −0.74 and

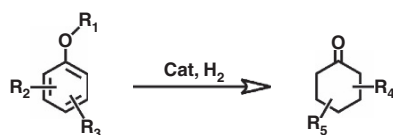
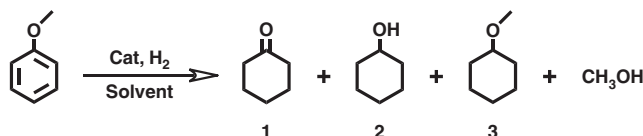


Figure 1 | A sustainable route to produce ketones from aromatic ethers.

Transformation of aromatic ethers with different substitute groups to corresponding ketones. R1, R2, R3, R4 and R5 stand for corresponding substitute groups.

Table 1 | Results for the transformation of anisole over noble metal catalyst at different conditions*.

Entry	Catalytic system [†]			t (h)	Conversion (%)	Selectivity (%)			Yield of 1 (%)
	Catalyst	Solvent	Additive			1	2	3	
1	Pd/C	CH ₂ Cl ₂	—	1.0	99.9	0.0	0.0	>99.0	0.0
2	Pd/C	<i>n</i> -C ₆ H ₁₄	—	1.0	45.5	0.0	0.0	>99.0	0.0
3	Pd/C	C ₂ H ₅ OH	—	1.0	23.5	0.0	0.0	>99.0	0.0
4	Pd/C	THF	—	1.0	8.6	0.0	0.0	>99.0	0.0
5	Pd/C	H ₂ O	—	2.5	99.8	13.0	43.3	42.5	13.0
6 [‡]	—	H ₂ O	—	2.5	0.0	0.0	0.0	0.0	0.0
7	Pt/C	H ₂ O	—	1.0	99.6	1.5	9.0	89.2	1.5
8	Ru/C	H ₂ O	—	1.0	99.6	0.0	19.2	80.7	0.0
9	Rh/C	H ₂ O	—	1.0	99.5	0.0	16.1	83.8	0.0
10 [§]	Pd/C	H ₂ O/CH ₂ Cl ₂	—	1.0	99.8	67.7	18.5	13.6	67.6
11 [§]	Pd/C	H ₂ O/C ₂ H ₅ OH	—	2.5	58.8	25.9	1.0	73.0	15.2
12 [§]	Pd/C	H ₂ O/THF	—	2.5	15.6	31.5	1.1	67.4	4.9
13	Pd/C	CH ₂ Cl ₂	KBr	2.5	99.9	0.0	0.0	>99.0	0.0
14 [¶]	Pd/C	H ₂ O	KBr	2.5	90.8	60.8	2.5	36.5	55.2
15 [#]	Pd/C	H ₂ O/CH ₂ Cl ₂	KBr	2.5	92.8	91.5	1.0	7.4	84.9
16 [#]	Pd/C	H ₂ O/CH ₂ Cl ₂	NaBr	2.5	94.6	88.9	1.8	9.2	84.1
17 [#]	Pd/C	H ₂ O/CH ₂ Cl ₂	KCl	2.5	99.8	68.5	17.2	14.1	68.4
18 [#]	Pd/C	H ₂ O/CH ₂ Cl ₂	KI	2.5	0.0	0.0	0.0	0.0	0.0
19 ^{**}	<i>m</i> -Pd/C	H ₂ O/CH ₂ Cl ₂	—	2.5	95.8	96.2	0.5	3.2	92.2
20 ^{**}	<i>m</i> -Pd/C	H ₂ O/CH ₂ Cl ₂	—	3.3	100.0	96.1	0.5	3.2	96.1
21 ^{††}	<i>m</i> -Pd/C	H ₂ O/CH ₂ Cl ₂	SiO ₂	2.5	96.0	96.0	0.6	3.2	92.2
22 ^{††}	<i>m</i> -Pd/C	H ₂ O/CH ₂ Cl ₂	CaCl ₂	2.5	95.2	96.5	0.4	3.0	91.9
23 ^{††}	<i>m</i> -Pd/C	H ₂ O/CH ₂ Cl ₂	K ₂ CO ₃	2.5	95.9	96.1	0.6	3.1	92.2
24 ^{††}	<i>m</i> -Pd/C	H ₂ O/CH ₂ Cl ₂	MgSO ₄	2.5	96.1	96.3	0.4	3.1	92.5

*Anisole (1.5 mmol), 90 °C, 2 MPa H₂.†5 wt% Pd/C, Pt/C, Ru/C, Rh/C, *m*-Pd/C (1.41 × 10⁻² mmol metals), volume of solvent (8.0 ml).‡Without catalyst and/or H₂.§H₂O/organic solvent (0.2 ml per 7.8 ml).

||KBr 0.5 mmol.

¶2.5 mol l⁻¹ KBr aqueous solution.#2.5 mol l⁻¹ salt aqueous solution (0.2 ml) + CH₂Cl₂ (7.8 ml).***m*-Pd/C was KBr modified Pd/C catalyst, and the content of Br⁻ is 0.3 mol% based on Pd (determined by ICP).††SiO₂ 0.3 mmol; salt 0.3 mmol.

– 0.26 eV, respectively (Supplementary Fig. 3). This suggests that anisole is more easily adsorbed on the surface of the catalyst and occupy the active site than cyclohexanone. So the anisole in the reaction system can prevent the adsorption of cyclohexanone on the catalyst and inhibit its hydrogenation to cyclohexanol, especially at higher anisole concentration. Thus, the DFT calculation can explain the phenomenon why the selectivity to cyclohexanone decreased quickly at higher anisole conversion (Supplementary Fig. 2a). Supplementary Fig. 2b shows the results of the reaction in H₂O/CH₂Cl₂. It can be known by comparing Supplementary Fig. 2a,b that selectivity with cyclohexyl methyl ether in H₂O/CH₂Cl₂ was lower than that in neat water. In other words, H₂O/CH₂Cl₂ solvent is not favourable to the generation of the by-product. Supplementary Fig. 2c shows the reaction results in KBr aqueous solution without CH₂Cl₂. It can be known by comparing Supplementary Fig. 2a,c that KBr could suppress the hydrogenation of cyclohexanone with cyclohexanol effectively, and could also reduce the selectivity to cyclohexyl methyl ether notably. To further confirm the effect of KBr, we conducted the hydrogenation of cyclohexanone in H₂O, H₂O/CH₂Cl₂, aqueous solution of KBr and H₂O/CH₂Cl₂ + KBr system under the same reaction conditions, and the results are presented in Supplementary Fig. 2d. Obviously, KBr was highly effective

to prevent the hydrogenation of cyclohexanone, especially in H₂O/CH₂Cl₂. From the results in Supplementary Fig. 2, we can conclude that H₂O/CH₂Cl₂ can inhibit the formation of cyclohexyl methyl ether, and KBr can prevent hydrogenation of cyclohexanone and suppress generation of cyclohexyl methyl ether. Therefore, the selectivity of cyclohexanone could be outstandingly high in H₂O/CH₂Cl₂ with KBr. It is well-known that Br⁻ can be adsorbed on Pd catalyst²⁸, which may be the main reason for the bromide salts to improve the selectivity of the reaction effectively. We carried out some experiments to verify this argument. In the experiments, the Pd/C catalyst was dispersed in KBr aqueous solution, and the mixture was stirred for 1 h. Then, *m*-Pd/C was obtained after filtration, washing, and drying. The adsorption of Br⁻ in the *m*-Pd/C was confirmed by the XPS (Supplementary Figs 4 and 5). The *m*-Pd/C was used to catalyse the reaction without adding additional KBr. And the selectivity to cyclohexanone could reach 96% (Table 1, entries 19 and 20), which was even higher than that when Pd/C was used with addition of KBr. This is understandable considering that in the latter case more by-product was formed at beginning because the adsorption of Br⁻ needs some time. SiO₂, CaCl₂, K₂CO₃ and MgSO₄ are the impurities of biomass-derived streams³³. Their effect on the reaction were also investigated (Table 1, entries 21–24). It

was demonstrated that the effect of the impurities on the catalytic performance of the catalytic system was not considerable. In the following, we study the effects of various conditions on the reaction in $\text{H}_2\text{O}/\text{CH}_2\text{Cl}_2$ over the Br- modified catalyst because they showed excellent performance.

Optimization of reaction conditions. The effects of amount of solvent used and H_2O content in $\text{H}_2\text{O}/\text{CH}_2\text{Cl}_2$ on the catalytic reaction over the m-Pd/C are shown in Fig. 2. The selectivity of cyclohexanone increased and that of cyclohexyl methyl ether decreased with the increase of the amount of solvent (Fig. 2a). However, the conversion of anisole decreased with increasing the volume of the solvent, which is understandable based on rate equation. Figure 2b demonstrates effect of H_2O content on the catalytic reaction. The conversion of anisole decreased continuously with increase of H_2O content in $\text{H}_2\text{O}/\text{CH}_2\text{Cl}_2$. This is understandable because the conversion of anisole in water was slower than in CH_2Cl_2 , as can be known from Table 1 (entries 1 and 5). The selectivity of cyclohexanone increased sharply with increasing H_2O content at the beginning from 0 to 2.5 v%, and then decreased gradually with further increase of H_2O content from 2.5 to 100 v%. The trend of the selectivity of cyclohexyl methyl ether was opposite to that of cyclohexanone. The selectivity of cyclohexanol increased slowly with increasing content of H_2O in the solvent. The results indicated that water is essential for the production of cyclohexanone. However, more water would promote the side reaction of the transformation of anisole to cyclohexyl methyl ether and the further hydrogenation of cyclohexanone to cyclohexanol.

The effects of temperature, H_2 pressure and reaction time on the conversion and product distribution of the reaction over the m-Pd/C in $\text{H}_2\text{O}/\text{CH}_2\text{Cl}_2$ are shown in Supplementary Fig. 6a–c. The results show that the optimized temperature and H_2 pressure were 90°C and 2 MPa, respectively. We also studied the reusability of the m-Pd/C. After reaction, the liquid was removed and the m-Pd/C catalyst was reused directly after washing and drying. The conversion of anisole and selectivity to cyclohexanone did not change notably after the catalyst was reused five times (Supplementary Fig. 6d). The m-Pd/C catalysts before and after using five times was also characterized by XPS, X-ray diffraction and TEM techniques. XPS spectra (Supplementary Figs 4 and 5) demonstrate that the Br^- adsorbed on the Pd surface was stable in the reaction process. The X-ray diffraction patterns (Supplementary Fig. 7) and TEM images (Supplementary Figs 1 and 8) indicate that the crystalline and particle size of the Pd nanoparticles did not change in the reaction. To further check the stability of the catalyst, the m-Pd/C catalyst in $\text{H}_2\text{O}/\text{CH}_2\text{Cl}_2$ was stirred at 120°C for 40 h (equivalent to the time for eight reaction cycles) in the absence of anisole. Then the catalyst was used for the reaction at the condition of entry 19 of Table 1. The conversion of anisole and selectivity to cyclohexanone were 95.0% and 96.6% respectively, which were nearly the same as that obtained using the virgin m-Pd/C catalyst, which further indicates the excellent stability of the m-Pd/C catalyst.

Reaction mechanism. It is well known that Pd can activate H_2 (ref. 34) and catalyse the partial hydrogenation of the benzene ring of phenol to an enol^{3,35}. To study the reaction mechanism, identification of intermediate in the transformation of anisole was carried out in this work, and 1-methoxycyclohexene was detected (Supplementary Fig. 9). On the basis of the experimental results in this work and the related knowledge in the literature, we propose the possible pathway of the reaction, which is shown schematically in Fig. 3. The benzene ring of anisole is first partially hydrogenated to form 1-methoxycyclohexene on

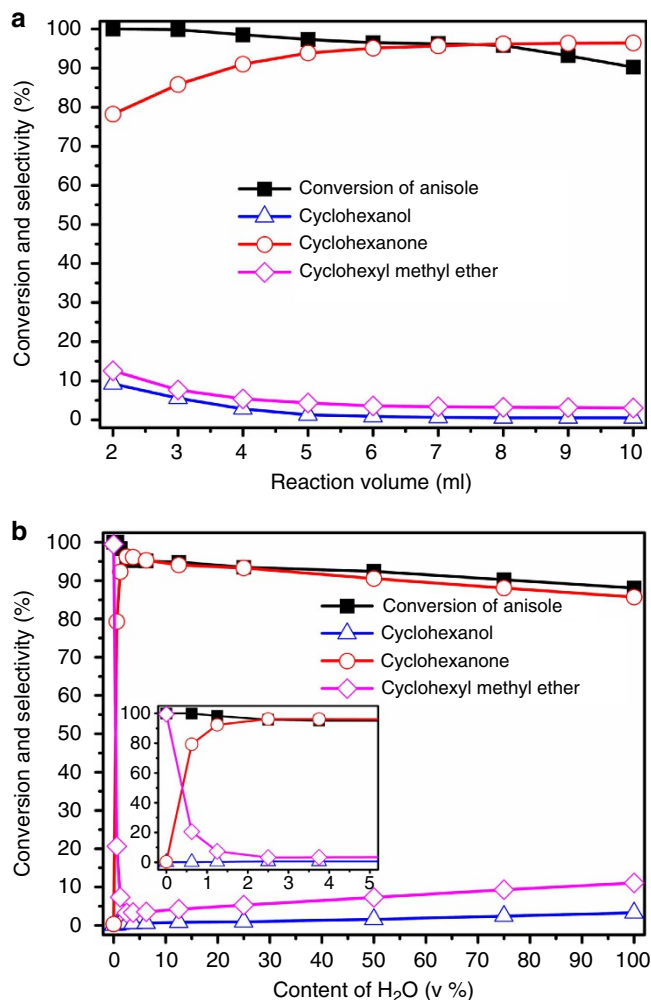


Figure 2 | Effects of solvent volume and content of water. Effects of solvent volume with a water amount of 0.2 ml (a) and content of H_2O at total solvent volume of 8.0 ml (b) on the conversion and product distribution of the reaction over m-Pd/C catalyst. Reaction conditions: anisole (1.5 mmol), 5 wt% m-Pd/C (0.03 g, 1.41×10^{-2} mmol Pd), 90°C , 2.5 h, 2 MPa.

Pd catalyst in Step 1, which can be further hydrogenated to cyclohexyl methyl ether (Step 2)³⁶ or hydrolysed to cyclohexanone (Steps 3–4)^{37,38}. Cyclohexanone can then be further hydrogenated to form cyclohexanol (Step 5). The experimental results support the proposed pathway. For example, cyclohexanone cannot be formed without water (Table 1), and the yield of methanol is similar to that of the total yield of the cyclohexanone and cyclohexanol (Supplementary Table 1), and no gaseous product was produced in the anisole transformation (Supplementary Fig. 10). All the results support the hydrolysis route (Steps 3–4). Besides, the isotope tracing experiment using H_2^{18}O indicated that only $\text{C}=\text{O}^{18}$ bond existed in cyclohexanone (Supplementary Fig. 11), further supporting the proposed pathway. Furthermore, we conducted the transformation of 1-methoxycyclohexene (Supplementary Fig. 12). It was shown that 1-methoxycyclohexene could be converted rapidly under reaction conditions and the product distribution was the same as that of anisole transformation.

Substrate scope. We also studied the catalytic performance of the m-Pd/C in $\text{H}_2\text{O}/\text{CH}_2\text{Cl}_2$ for the conversion of other

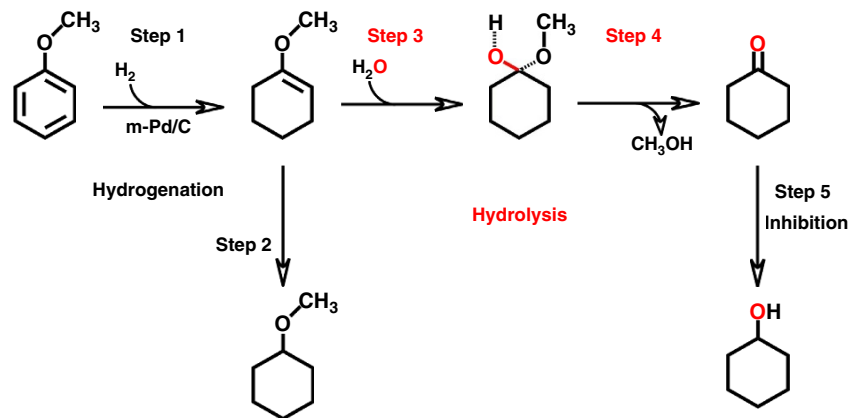


Figure 3 | Proposed reaction pathway for the transformation of anisole over the m-Pd/C catalyst in H₂O/CH₂Cl₂ medium. The benzene ring of anisole is first partially hydrogenated to form 1-methoxycyclohexene on Pd catalyst in Step 1, which can be further hydrogenated to cyclohexyl methyl ether (Step 2) or hydrolysed to cyclohexanone (Steps 3–4). Cyclohexanone can then be further hydrogenated to form cyclohexanol (Step 5). The m-Pd/C and H₂O/CH₂Cl₂ catalytic system promoted the production of cyclohexanone and inhibited the production of cyclohexyl methyl ether and cyclohexanol.

aromatic ethers to cyclohexanone or its corresponding derivatives. Table 2 gives the optimized reaction conditions and the yields of corresponding desired products for various substrates. In general, the catalytic system was more efficient for anisole derivatives with electron-donating substituents than those with electron-withdrawing substituents (Table 2, entries 1–14). 4-Methyl anisole (Table 2, entry 1) and 2-methyl anisole (Table 2, entry 2) could be converted to 4-methyl cyclohexanone and 2-methyl cyclohexanone with the yields of 80.1% and 90.3%, respectively. 4-Ethyl anisole (Table 2, entry 3) and 2-ethyl anisole (Table 2, entry 4) could be converted to 4-ethyl cyclohexanone and 2-ethyl cyclohexanone and the yields were 81.5% and 88.1%, respectively. Moreover, 2-methoxyphenol, 2-methoxy-4-methylphenol, and 4-ethyl-2-methoxyphenol can be produced from depolymerization of lignin¹⁵. They could be converted to the corresponding ketones in this catalytic system, and the overall yields of the ketones were 64.8% (Table 2, entry 5), 74.2% (Table 2, entry 6) and 60.2% (Table 2, entry 7), respectively. Anethole and *trans*-anethole exist widely in anise, fennel and tarragon, which can be extracted^{21–23}. Anethole (Table 2, entry 8) and *trans*-anethole (Table 2, entry 9) could be converted into 4-propylcyclohexanone with yields of 77.3% and 71.8%, respectively. However, anisole with electron-withdrawing substituents such as ester group, trifluoromethyl group and formyl group afforded low yield of ketone product (Table 2, entries 10–14). The yield of 3-oxo-cyclohexanecarboxylic acid methyl ester was 41.6% (Table 2, entry 10). When ester group was on para-position, the yield of desired product decreased to 35.1% (Table 2, entry 11). The yield of 3-(trifluoromethyl) cyclohexanone was 15.1% and the yield of 4-(trifluoromethyl) cyclohexanone was 0% (Table 2, entries 12 and 13). Formyl substitute afforded 0% yield of the desired product (Table 2, entry 14). In addition, the catalytic system could also catalyse the transformation of benzyl phenyl ether and diphenyl ether that represent typical ethers with α -O-4 and 4-O-5 linkages in lignin and are typical lignin-derived compounds^{13,14} to cyclohexanone, and the yields of cyclohexanone could reach 93.0% and 94.2%, respectively (Table 2, entries 15 and 16).

Discussion

m-Pd/C in H₂O/CH₂Cl₂ can catalyse the transformation of aromatic ethers to cyclohexanone or its corresponding derivatives via hydrogenation and hydrolysis processes, and high to

moderate yield of the corresponding ketones can be obtained. In general, the catalytic system is more efficient for anisole derivatives with electron-donating substituents than those with electron-withdrawing substituents. Detailed study indicates that m-Pd/C and H₂O/CH₂Cl₂ cooperatively promote the partial hydrogenation to vinyl ethers and their hydrolysis to ketones, and the bromide anions adsorbed on the surface of Pd catalyst inhibit the hydrogenation of ketones and suppress generation of byproduct. Thus, the selectivity to the desired ketone products can be very high. In addition, m-Pd/C can be reused at least five times without reducing the activity and selectivity notably, indicating that the catalytic system is very stable. Aromatic ethers can be extracted from some plants directly. In addition, study on depolymerization of lignin to produce low-molecular-weight compounds is receiving increasing attention in recent years, and more and more aromatic ethers may be produced from lignin in the future. We believe that the route reported in this work has great potential of application for producing ketones sustainably.

Methods

Materials. Anisole (99.0%), cyclohexanol (99.0%), 2-cyclohexylethanol (99.0%), biphenyl (99.0%), phenol (99.0%), cesium bromide (99.9%), diphenyl ether (99%), 2-methoxy-4-methylphenol (98%), 4-ethyl-2-methoxyphenol (98%), 4-ethylanisole (98%), 4-(trifluoromethyl)cyclohexanone (97%) and silicon oxide were purchased from Alfa Aesar. Guaiacol (99.0%), (E)-1-methoxy-4-(prop-1-en-1-yl), benzene (*trans*-anethole) (99.0%), 2-methylanisole (99.0%), 4-methylanisole (99.0%), 2-methylcyclohexanone (98.0%), 4-methylcyclohexanone (98.0%) and 3-methylcyclohexanone (97.0%) were purchased from Acros Organics. 1-Methoxy-4-(prop-1-en-1-yl) benzene (*cis*-anethole) (97.0%), 4-ethylcyclohexanone (95.0%), 4-hydroxycyclohexanone (99.0%) and 1-methoxy-4-(trifluoromethyl)benzene (95%) were purchased from Ark Pharm. 2-Ethylanisole (98%), methylcyclohexane (99.0%), ethylcyclohexane (98.0%), methoxycyclohexane (98.0%), benzyl phenyl ether (98.0%), 4-propylcyclohexanone (98.0%), 4-propylcyclohexanol (98.0%) and 2-methoxycyclohexanone (95.0%) were obtained from TCI (Shanghai) Development Co., Ltd. 4-Propylanisole (99.0%), 3-(trifluoromethyl)anisole (99%), 4-methoxybenzamide (97%), methyl 4-methoxybenzoate (99%), methyl 3-methoxybenzoate (98%), methyl 2-methoxybenzoate (97%), 2-methoxycarbonylcyclohexanone (90%) and H₂¹⁸O (97 atom% ¹⁸O) were purchased from J & K Scientific Ltd. Chloroform-D (D, 99.8% + 3% v/v TMS) was purchased from Cambridge Isotope Laboratories, Inc. Potassium bromide (99.0%), potassium chloride (99.5%), potassium iodide (99.0%), sodium bromide (A. R.), Magnesium sulfate anhydrous (98.0%), calcium chloride anhydrous (96.0%), potassium carbonate anhydrous (99.0%), *n*-hexane (A. R.), tetrahydrofuran (A. R.), 2-phenylethyl bromide (99.0%), toluene (99.5%) and ethylbenzene (98.5%) were obtained from Sinopharm Chemical Reagent Co., Ltd. Methanol (99.9%) ethanol (99.9%), ethyl acetate (99.5%), dichloromethane (99.5%), cyclohexanone (99.5%) and cyclohexane (99.5%) were obtained from the Beijing Chemical Company. 1-Methoxycyclohexene (a mixture of 50 mol% 1-methoxycyclohexene and 50 mol%

Table 2 | Transformation of different substrates to cyclohexanone and its derivatives*.

Entry	Substrate	m-Pd/C (mg)	Reaction conditions		Medium (ml)		Distribution and yield (%) of Ketones
			T (°C)	t (h)	H ₂ O	CH ₂ Cl ₂	
1		30	90	8	0.2	5.0	 80.1
2		30	90	8	0.2	5.0	 90.3
3		30	90	8	0.2	5.0	 81.5
4		30	90	8	0.2	5.0	 88.1
5		45	130	15	0.5	4.0	 15.8, 38.8, 10.2
6		50	140	15	0.5	4.0	 12.2, 17.9, 15.6, 5.8, 7.5, 15.2
7		50	140	15	0.5	4.0	 5.5, 14.0, 11.8, 28.9
8		30	90	12	0.2	5.0	 77.3
9		30	90	12	0.2	5.0	 71.8
10 [†]		50	130	20	0.2	4.0	 41.6
11 [†]		50	130	20	0.2	4.0	 35.1
12 [†]		50	140	20	0.2	3.0	 15.1
13 [‡]		50	140	20	0.2	3.0	 0
14 [‡]		50	140	20	0.2	3.0	 0
15		35	90	8	0.2	5.0	 93.0, 42.2, 56.6
16		40	90	10	0.2	5.0	 94.2, 92.5

*Yield of products at full conversion of substrates, as averages of three experiments conducted in parallel. Substrate (1.0 mmol), H₂ (2.0 MPa).[†]Conversion of methyl 3-methoxybenzoate, methyl 4-methoxybenzoate and 3-(trifluoromethyl) anisole, 65.8, 50.1 and 18.8%.[‡]Conversion of 1-methoxy-4-(trifluoromethyl) benzene and 4-methoxybenzamide, 0%.

cyclohexanone dimethylacetal) was purchased from Toronto Research Chemicals. Nitrogen (>99.99%) and hydrogen (>99.99%) were provided by Beijing Analytic Instrument Company.

Catalysts and characterization. Pd/C (5 wt% Pd), Pt/C (5 wt% Pt), Rh/C (5 wt% Rh) were purchased from Alfa Aesar. Ru/C (5 wt% Ru) was obtained from TCI (Shanghai) Development Co., Ltd. m-Pd/C catalyst was prepared in a 50 ml Teflon-lined stainless-steel reactor equipped with a stirrer. In a typical experiment, 0.1 g Pd/C catalyst (5 wt% Pd), 25 ml KBr aqueous solution (0.1 mol l⁻¹) were added into the reactor. The reactor was sealed and purged with N₂ to remove the air in the reactor. After stirring for 1 h at 30 °C, the solid Pd/C catalyst was recovered by filtration, followed by washing using ethanol aqueous solution of 20 v% ethanol (5 × 10 ml), and then was washed with 10 ml water. Finally, the Pd/C catalyst recovered by filtration was dried at 100 °C in a vacuum oven for 5 h, and the modified catalyst is named as m-Pd/C.

The catalysts were characterized by X-ray diffraction, X-ray photoelectron spectroscopy (XPS), transmission electron microscopy (TEM), and high-resolution TEM (HRTEM), inductively Coupled Plasma-Atomic Emission Spectroscopy (ICP-AES) techniques. X-ray diffraction measurements were conducted on an X-ray diffractometer (D/MAX-RC, Japan) operated at 40 kV and 200 mA with Cu K α (λ = 0.154 nm) radiation. TEM and HRTEM images were measured on a JEOL-2011F electron microscope operating at 200 kV. Before measurement, the catalyst was ground, suspended in ethanol, and dispersed by ultrasonic treatment. The obtained dispersion was transferred to a copper-grid-supported carbon film. The XPS measurements were carried out on an ESCAL Lab 220i-XL spectrometer at a pressure of $\sim 3 \times 10^{-9}$ mbar (1 mbar = 100 Pa) using Al K α as the excitation source ($h\nu$ = 1486.6 eV) and operated at 15 kV and 20 mA. The contents of bromide anions adsorbed on the m-Pd/C catalysts were determined by ICP.

Reaction. The reaction was carried out in a Teflon-lined stainless-steel reactor of 20 ml with a magnetic stirrer. The reactor was connected to a hydrogen cylinder of the reaction pressure, so that hydrogen of fixed pressure could be supplied continuously. The pressure was determined by a pressure transducer (FOXBORO/ICT, Model 93), which could be accurate to ± 0.025 MPa. In a typical experiment, suitable amount of reactant, catalyst, solvent and salt (if used) were loaded into the reactor. The reactor was sealed and purged with hydrogen to remove the air at room temperature. Then the reactor was placed in a furnace at desired temperature. Hydrogen was introduced into the reactor and the stirrer was started with a stirring speed of 800 r.p.m. After the reaction, the reactor was placed in ice water and the gas was released and collected in a gas bag that was purged with H₂ five times. The gaseous sample was analysed using a GC (Agilent 4890D) equipped with a TCD detector and a packed column (Carbon molecular sieve TDX-01, 1 m in length and 3 mm in diameter) using Argon as the carry gas. A known amount of internal standard (biphenyl) was added into the reactor. The liquid reaction mixture in the reactor was transferred into a centrifuge tube. The reactor was washed using ethyl acetate, which was combined the reaction mixture. The catalyst was separated by centrifugation. The quantitative analysis of the liquid products was conducted using a GC (Agilent 6820) equipped with a flame ionization detector (FID) and a HP-5MS capillary column (0.25 mm in diameter, 30 m in length). Identification of the products and reactant was done using a GC-MS (Agilent 5977A, HP-5MS capillary column (0.25 mm in diameter, 30 m in length)) as well as by comparing the retention time with respective standards in GC traces. The conversion of anisole and selectivities of the products were calculated from the GC data.

Recycling of the catalyst. The reusability of m-Pd/C catalyst was tested for anisole transformation in H₂O/CH₂Cl₂ system. After the reaction, the reaction mixture was centrifuged and the solid m-Pd/C catalyst was recovered by filtration, followed by washing using ethanol aqueous solution of 20 v% ethanol (5 × 10 ml), and then was washed with 10 ml water. The m-Pd/C catalyst was reused directly for the next run after drying at 100 °C for 5 h in a vacuum oven. To further check the stability of the catalyst, the m-Pd/C catalyst in H₂O/CH₂Cl₂ was stirred at 120 °C for 40 h without anisole, which was equivalent to 8 cycles. After the stirring, the mixture was centrifuged and the solid m-Pd/C catalyst was recovered by filtration, followed by washing using ethanol aqueous solution of 20 v% ethanol (5 × 10 ml), and then was washed with 10 ml water. The m-Pd/C catalyst was reused for anisole transformation in H₂O/CH₂Cl₂ system after drying at 100 °C for 5 h in a vacuum oven.

¹⁸O isotope labelling of cyclohexanone. The reactor used was the same as that described above. In the experiment, 1.5 mmol anisole, 0.03 g m-Pd/C, 0.2 ml H₂¹⁸O and 7.8 ml CH₂Cl₂ were loaded into the reactor. The reactor was sealed and purged with hydrogen to remove the air at room temperature. Then the reactor was placed in a furnace at 90 °C. 2 MPa H₂ was introduced into the reactor and the stirrer was started with a stirring speed of 800 r.p.m. After the reaction, the reactor was placed in ice water and the gas was released. The reaction mixture was transferred into a centrifuge tube and the catalyst was separated by centrifugation. Identification of the ¹⁸O-cyclohexanone was detected using a GC-MS (Agilent 5977A).

Computational details. DFT calculations were performed with the Vienna *Ab initio* Simulations Package (VASP) code³⁹. The electron exchange and correlation energy were modified within the generalized gradient approximation (GGA) in the Perdew-Burke-Ernzerhof formalism (PBE)⁴⁰. Core electron interactions were described with the projector-augmented wave (PAW) method⁴⁰. The methods used have been applied to DFT studies of arene derivatives and surface sites of Pd nanoparticles⁴¹.

In this work, the slab Pd (111) surface was used to represent the surface of Pd nanoparticles. Four layers (4 × 4) Pd (111) was used, in which the first two layers with adsorbates were relaxed, and the two bottom layers were fixed during the optimization and the vacuum layer of Pd (111) was 15 Å. The Brillouin zone integration was employed using a Monkhorst-Pack grid with 4 × 4 × 1 for the slab Pd (111)⁴². The cutoff energy for the plane waves was set up to 400 eV and the smearing width was 0.2 eV. Force convergence was set to be lower than 0.02 eV/Å, and total energy convergence was set to be less than 10⁻⁴ eV.

The adsorption energy of molecule on the slab Pd (111) surface was calculated as follows:

$$E_{\text{ads}} = E_{\text{molecule + slab}} - E_{\text{molecule}} - E_{\text{slab}} \quad (1)$$

where E_{ads} , $E_{\text{molecule + slab}}$, E_{molecule} and E_{slab} represents the adsorption energy, the total energy after molecule is adsorbed on the slab Pd (111) surface, the energy of isolated molecule, and the total energy of the slab, respectively⁴¹.

Data availability. All relevant data are available from the authors on reasonable request.

References

- Wang, Y., Yao, J., Li, H. R., Su, D. S. & Antonietti, M. Highly selective hydrogenation of phenol and derivatives over a Pd@Carbon nitride catalyst in aqueous media. *J. Am. Chem. Soc.* **133**, 2362–2365 (2011).
- Sun, H., Blatter, F. & Frei, H. Cyclohexanone from cyclohexane and O₂ in a zeolite under visible light with complete selectivity. *J. Am. Chem. Soc.* **118**, 6873–6879 (1996).
- Liu, H. Z., Jiang, T., Han, B. X., Liang, S. G. & Zhou, Y. X. Selective phenol hydrogenation to cyclohexanone over a dual supported Pd-Lewis acid catalyst. *Science* **326**, 1250–1252 (2009).
- Hajra, A., Wei, Y. & Yoshikai, N. Palladium-catalyzed aerobic dehydrogenative aromatization of cyclohexanone imines to arylamines. *Org. Lett.* **14**, 5488–5491 (2012).
- Banon-Caballero, A., Guillena, G. & Najera, C. Solvent-free enantioselective friedlander condensation with wet 1, 1'-binaphthalene-2, 2'-diamine-derived prolinamides as organocatalysts. *J. Org. Chem.* **78**, 5349–5356 (2013).
- Patino, P. *et al.* Oxidation of cycloalkanes and diesel fuels by means of oxygen low pressure plasmas. *Energy Fuels* **16**, 1470–1475 (2002).
- Meyers, A. I., Williams, D. R., Erickson, G. W., White, S. & Druelinger, M. Enantioselective alkylation of ketones via chiral, nonracemic lithioenamines. An asymmetric synthesis of α -alkyl and α, α' -dialkyl cyclic ketones. *J. Am. Chem. Soc.* **103**, 3081–3087 (1981).
- He, M. Y., Sun, Y. H. & Han, B. X. Green carbon science: scientific basis for integrating carbon resource processing, utilization, and recycling. *Angew. Chem. Int. Ed.* **52**, 9620–9633 (2013).
- Zakzeski, J., Bruijninx, P. C. A., Jongerijs, A. L. & Weckhuysen, B. M. The catalytic valorization of lignin for the production of renewable chemicals. *Chem. Rev.* **110**, 3552–3599 (2010).
- Ragauskas, A. J. *et al.* Lignin valorization: improving lignin processing in the biorefinery. *Science* **344**, 709–719 (2014).
- Tuck, C. O., Perez, E., Horvath, I. T., Sheldon, R. A. & Poliakov, M. Valorization of biomass: deriving more value from waste. *Science* **337**, 695–699 (2012).
- He, J. Y., Zhao, C. & Lercher, J. A. Ni-catalyzed cleavage of aryl ethers in the aqueous phase. *J. Am. Chem. Soc.* **134**, 20768–20775 (2012).
- Ohlrogge, J. *et al.* Driving on biomass. *Science* **324**, 1019–1020 (2009).
- Sanderson, K. Lignocellulose: a chewy problem. *Nature* **474**, S12–S14 (2011).
- Ma, R., Hao, W. Y., Ma, X. L., Tian, Y. & Li, Y. D. Catalytic ethanolysis of kraft lignin into high-value small-molecular chemicals over a nanostructured α -molybdenum carbide catalyst. *Angew. Chem. Int. Ed.* **53**, 7310–7315 (2014).
- Rahimi, A., Ulbrich, A., Coon, J. J. & Stahl, S. S. Formic-acid-induced depolymerization of oxidized lignin to aromatics. *Nature* **515**, 249–252 (2014).
- Rinaldi, R. *et al.* Paving the way for lignin valorisation: recent advances in bioengineering, biorefining and catalysis. *Angew. Chem. Int. Ed.* **55**, 8164–8215 (2016).
- Gao, F., Webb, J. D. & Hartwig, J. F. Chemo- and regioselective hydrogenolysis of diaryl ether C-O bonds by a robust heterogeneous Ni/C catalyst: applications to the cleavage of complex lignin-related fragments. *Angew. Chem. Int. Ed.* **55**, 1474–1478 (2016).

19. Deuss, P. J. *et al.* Aromatic Monomers by *in Situ* Conversion of reactive intermediates in the acid-catalyzed depolymerization of lignin. *J. Am. Chem. Soc.* **137**, 7456–7467 (2015).
20. Li, C. Z., Zhao, X. C., Wang, A. Q., Huber, G. W. & Zhang, T. Catalytic transformation of lignin for the production of chemicals and fuels. *Chem. Rev.* **115**, 11559–11624 (2015).
21. O'Shea, S. K., Von Riesen, D. D. & Rossi, L. L. Isolation and analysis of essential oils from spices. *J. Chem. Educ.* **89**, 665–668 (2012).
22. Lummiss, J. A. M. *et al.* Chemical plants: high-value molecules from essential oils. *J. Am. Chem. Soc.* **134**, 18889–18891 (2012).
23. Obolskiy, D., Pischel, I., Feistel, B., Glotov, N. & Heinrich, M. *Artemisia dracunculus* L. (Tarragon): a critical review of its traditional use, chemical composition, pharmacology, and safety. *J. Agric. Food Chem.* **59**, 11367–11384 (2011).
24. Runnebaum, R. C., Lobo-Lapudis, R. J., Nimmanwudipong, T., Block, D. E. & Gates, B. C. Conversion of anisole catalyzed by platinum supported on alumina: the reaction network. *Energy Fuels* **25**, 4776–4785 (2011).
25. Hubert, C., Denicourt-Nowicki, A., Guegan, J. P. & Roucoux, A. Polyhydroxylated ammonium chloride salt: a new efficient surfactant for nanoparticles stabilisation in aqueous media. Characterization and application in catalysis. *Dalton Trans.* **36**, 7356–7358 (2009).
26. Chinta, S. & Lunsford, J. H. A mechanistic study of H₂O₂ and H₂O formation from H₂ and O₂ catalyzed by palladium in an aqueous medium. *J. Catal.* **225**, 249–255 (2004).
27. Liu, Q. S., Bauer, J. C., Schaak, R. E. & Lunsford, J. H. Supported palladium nanoparticles: an efficient catalyst for the direct formation of H₂O₂ from H₂ and O₂. *Angew. Chem. Int. Ed.* **47**, 6221–6224 (2008).
28. Choudhary, V. R. & Samanta, C. Role of chloride or bromide anions and protons for promoting the selective oxidation of H₂ by O₂ to H₂O₂ over supported Pd catalysts in an aqueous medium. *J. Catal.* **238**, 28–38 (2006).
29. Edwards, J. K. & Hutchings, G. J. Palladium and gold-palladium catalysts for the direct synthesis of hydrogen peroxide. *Angew. Chem. Int. Ed.* **47**, 9192–9198 (2008).
30. Tan, Y. P. *et al.* Catalyst-induced changes in a substituted aromatic: A combined approach via experiment and theory. *Surf. Sci.* **589**, 173–183 (2005).
31. Rasmussen, A. M. H. & Hammer, B. Adsorption, mobility, and dimerization of benzaldehyde on Pt (111). *J. Chem. Phys.* **136**, 174706–174714 (2012).
32. Bonalumi, N., Vargas, A., Ferri, D. & Baiker, A. Theoretical and spectroscopic study of the effect of ring substitution on the adsorption of anisole on platinum. *J. Phys. Chem. B* **110**, 9956–9965 (2006).
33. Huber, G. W., Iborra, S. & Corma, A. Synthesis of transportation fuels from biomass: chemistry, catalysts, and engineering. *Chem. Rev.* **106**, 4044–4098 (2006).
34. Benkhaled, M. *et al.* Study of hydrogen surface mobility and hydrogenation reaction over alumina-supported palladium catalysts. *Appl. Catal. A* **346**, 36–43 (2008).
35. Zhuang, L., Li, H. X., Dai, W. L. & Qiao, M. H. Liquid phase hydrogenation of phenol to cyclohexenone over a Pd-La-B amorphous catalyst. *Chem. Lett.* **32**, 1072–1073 (2003).
36. Widegren, J. A. & Finke, R. G. Anisole hydrogenation with well-characterized polyoxoanion- and tetrabutylammonium-stabilized Rh (0) nanoclusters: effects of added water and acid, plus enhanced catalytic rate, lifetime, and partial hydrogenation selectivity. *Inorg. Chem.* **41**, 1558–1572 (2002).
37. Kresge, A. J., Sagatys, D. S. & Chen, H. L. Vinyl ether hydrolysis. 9. Isotope effects on proton transfer from the hydronium ion. *J. Am. Chem. Soc.* **99**, 7228–7233 (1977).
38. Brynes, S. D. & Fedor, L. R. Vinyl ether hydrolysis. II. General acid catalyzed hydration of 3-alkoxy- and 3-aryloxycrotonic acid derivatives. *J. Am. Chem. Soc.* **94**, 7016–7019 (1972).
39. Luo, Q. Q., Wang, T., Beller, M. & Jiao, H. J. Acrolein hydrogenation on Ni (111). *J. Phys. Chem. C* **117**, 12715–12724 (2013).
40. Perdew, J. P., Bruke, K. & Ernzerhof, M. Generalized gradient approximation made simple. *Phys. Rev. Lett.* **77**, 3865–3868 (1996).
41. He, X. B. *et al.* Density functional theory study of p-chloroaniline adsorption on Pd surfaces and clusters. *Int. J. Quantum Chem.* **114**, 895–899 (2014).
42. Monkhorst, M. & Pack, J. D. Special points for Brillouin-zone integrations. *Phys. Rev. B* **13**, 5188–5192 (1976).

Acknowledgements

The work was supported by National Natural Science Foundation of China (21133009, 21603235, 21673249), the Recruitment Program of Global Youth Experts of China, and Chinese Academy of Sciences (QYZDY-SSW-SLH013).

Author contributions

Q.M., H.L. and B.H. proposed the project, designed and conducted the experiments and wrote the manuscript. Other authors performed some experiments and discussed the work.

Additional information

Supplementary Information accompanies this paper at <http://www.nature.com/naturecommunications>

Competing financial interests: The authors declare no competing financial interests.

Reprints and permission information is available online at <http://npj.nature.com/reprintsandpermissions/>

How to cite this article: Meng, Q. *et al.* Synthesis of ketones from biomass-derived feedstock. *Nat. Commun.* **8**, 14190 doi: 10.1038/ncomms14190 (2017).

Publisher's note: Springer Nature remains neutral with regard to jurisdictional claims in published maps and institutional affiliations.



This work is licensed under a Creative Commons Attribution 4.0 International License. The images or other third party material in this article are included in the article's Creative Commons license, unless indicated otherwise in the credit line; if the material is not included under the Creative Commons license, users will need to obtain permission from the license holder to reproduce the material. To view a copy of this license, visit <http://creativecommons.org/licenses/by/4.0/>

© The Author(s) 2017